Spin gaps and bilayer coupling in $YBa_2Cu_3O_{7-\delta}$ and $YBa_2Cu_4O_8$

A. J. Millis
AT&T Bell Laboratories, 600 Mountain Avenue, Murray Hill, New Jersey 07974

H. Monien*
Institute for Theoretical Physics, University of California, Santa Barbara, California 93106
(Received 27 October 1993)

We investigate the relevance to the physics of underdoped $YBa_2Cu_3O_{6+x}$ and $YBa_2Cu_4O_8$ of the quantum critical point which occurs in a model of two antiferromagnetically coupled planes of antiferromagnetically correlated spins. We use a Schwinger boson mean-field theory and a scaling analysis to obtain the phase diagram of the model and the temperature and frequency dependence of various susceptibilities and relaxation rates. We distinguish between a low ω, T coupled-planes regime in which the optic spin excitations are frozen out and a high ω, T decoupled-planes regime in which the two planes fluctuate independently. In the coupled-planes regime the yttrium nuclear relaxation rate at low temperatures is larger relative to the copper and oxygen rates than would be naively expected in a model of uncorrelated planes. Available data suggest that in $YBa_2Cu_4O_8$ the crossover from the coupled to the decoupled planes regime occurs at $T > 700$ K or $T \sim 200$ K. The predicted correlation length is of order six lattice constants at $T = 200$ K. Experimental data related to the antiferromagnetic susceptibility of $YBa_2Cu_4O_8$ may be made consistent with the theory, but available data for the uniform susceptibility are inconsistent with the theory.

I. INTRODUCTION

In this paper we investigate the relevance to the physics of underdoped $YBa_2Cu_3O_{6+x}$ and $YBa_2Cu_4O_8$ of a $T=0$ order-disorder transition which occurs in a model of two antiferromagnetically coupled planes of antiferromagnetically correlated spins. This transition might be relevant because (a) in these compounds the basic structural unit is a pair of CuO_2 planes separated from each other by the relatively inert CuO chains,[1] (b) there is evidence for strong antiferromagnetic correlations within a CuO_2 plane,[2-4] (c) neutron scattering experiments find that for all ω and T studied a spin in one plane is perfectly anticorrelated with the nearest-neighbor spin on the nearest-neighbor plane,[4,5] (d) for $T < 150$ K both the static uniform susceptibility and the various NMR relaxation rates drop rapidly as T decreases[6] suggesting[7-9] that the system is evolving as T is decreased towards a quantum disordered ground state with a gap to spin excitations, and (e) the spin physics of $La_{2-x}Sr_xCuO_4$, in which the CuO_2 planes are very weakly coupled, is apparently rather different,[7] suggesting that the behavior of $YBa_2Cu_3O_{6+x}$ may be due at least in part to a coupling between planes. A preliminary version of this work was published previously.[7]

The model we consider is a Heisenberg model of spins sitting on sites of the lattice depicted in Fig. 1 and has two coupling constants, both taken to be antiferromagnetic. One, J_1, couples nearest-neighbor spins in the same plane. The other, J_2, couples a spin in one plane to the nearest spin in the other plane. The Hamiltonian is

$$H = J_1 \sum_{\langle i,j \rangle, a} \mathbf{S}_i^{(a)} \cdot \mathbf{S}_j^{(a)} + J_2 \sum_i \mathbf{S}_i^{(1)} \cdot \mathbf{S}_i^{(2)} . \quad (1.1)$$

Here i labels sites in a given plane, i and j are nearest neighbors in the same plane, and $a = 1,2$ labels two planes. There are two dimensionless parameters J_2/J_1 and S, the magnitude of the spin. At temperature $T=0$, Eq. (1.1) has two phases. One is antiferromagnetically ordered; the other is a singlet phase with a gap to excitations and no long-range order. Varying J_2/J_1 and S produces transitions between the phases. In a physical Heisenberg model S would take only half-integer or integer values $\frac{1}{2}, 1, \frac{3}{2}, \ldots$. However, it is interesting to consider values $S < \frac{1}{2}$ because the singlet phases occurring for small S in this model may be useful representations of the "spin-gap" behavior occurring in the underdoped $YBa_2Cu_3O_{6+x}$. We shall determine the phase diagram and discuss the physical properties at the transition and on the disordered side. The $T=0$ transition is in the universality class of the $(2+1)$-dimensional Heisenberg model and some universal properties have been determined.[10,11] Here, we pay particular attention to the effects of the interplane coupling J_2. We show that one

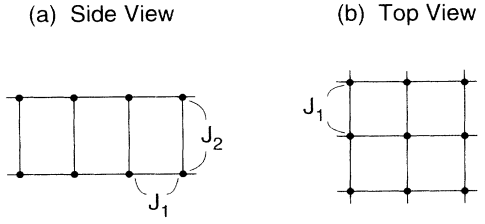

FIG. 1. Model system considered in this paper: two square arrays of spins with in-plane coupling J_1 and between-plane coupling J_2.

0163-1829/94/50(22)/16606(17)/$06.00

must distinguish between a low-ω, T "coupled-planes" regime and a high-ω, T "decoupled-planes regime." In the coupled-planes regime, one linear combination (essentially the optic mode of the spin excitation spectrum) is frozen out and the low energy physics is determined by acoustic spin fluctuations in which moments in the two planes fluctuate coherently. In the decoupled planes regime the two planes fluctuate essentially independently. One important feature of the quantum critical point considered here is the close relationship between the susceptibility at small q and at a q near the ordering wave vector.[11] We show that this, when combined with interplanar coupling, has a surprising implication for the yttrium relaxation rate: In the coupled-planes regime it is larger, relative to the other rates, than one would expect from a model of uncoupled planes.

We emphasize that Eq. (1.1) is not a completely realistic model of $YBa_2Cu_3O_{6.6}$ or $YBa_2Cu_4O_8$ because it omits the itinerant carriers which make these materials metallic and indeed superconducting. The itinerant carriers also strongly affect the magnetism. In all of the hole-doped CuO_2 compounds, long-range magnetic order disappears essentially at the metal-insulator transition.[12] It therefore seems likely that the itinerant carriers substantially weaken the in-plane magnetic correlations. Itinerant carriers also presumably give rise to a particle-hole continuum of incoherent spin excitations which may strongly affect the physics and which in appropriate circumstances may change the universality class of the transition.[13,14] It has, however, recently been argued that there is some evidence that the behavior of $YBa_2Cu_3O_{6.6}$ and $YBa_2Cu_4O_8$ is in the universality class of Eq. (1.1).[9]

The rest of the paper is organized as follows. In Sec. II we solve Eq. (1.1) via the Schwinger-boson mean-field theory. In Sec. III we give the results of the Schwinger-boson mean-field theory for the phase diagram and the physical susceptibilities relevant to NMR and neutron scattering experiments. In Sec. IV we combine selected results of the mean-field theory with other arguments to map the problem onto a recently constructed scaling theory of the transition[11] and give the relevant results of the scaling analysis. Section V is a conclusion in which we discuss the results and their relation to experiments on $YBa_2Cu_3O_{6.6}$ and $YBa_2Cu_4O_8$. It may be read independently of the previous sections by readers uninterested in the derivations of the results. Appendixes present details of various calculations.

II. MEAN-FIELD SOLUTION

We first study Eq. (1.1) by the Schwinger-boson mean-field method.[15] In this method one introduces Bose operators $b_{i\alpha}^{\dagger(a)}$ which create a state of spin α on site i of plane a. One restricts oneself to the subspace in which each site on each plane has $2S$ bosons, corresponding to spin S; thus we enforce the constraint

$$\sum_a b_{i\alpha}^{\dagger(a)} b_{i\alpha}^{(a)} = 2S \ . \tag{2.1}$$

A spin operator is written

$$\mathbf{S}_i^{(a)} = \sum_{\alpha\beta} b_{i\alpha}^{\dagger(a)} \sigma_{\alpha\beta} b_{i\beta}^{(a)} \ . \tag{2.2}$$

We now substitute Eq. (2.2) into Eq. (1.1). Then on the even sublattice of plane 1 and the odd sublattice of plane 2 we make the time reversal transformation which in the $S=\frac{1}{2}$ case is

$$\begin{aligned} b_\uparrow^\dagger &\to -b_\downarrow^\dagger \ , \\ b_\downarrow^\dagger &\to b_\uparrow^\dagger \ . \end{aligned} \tag{2.3}$$

Rearranging and using Eq. (2.1) leads to

$$\begin{aligned} H' = &-\frac{1}{2} J_1 \sum_{\langle i,j\rangle a\alpha\beta} (b_{i,\alpha}^{\dagger(a)} b_{j,\alpha}^{\dagger(a)})(b_{i\beta}^{(a)} b_{j,\beta}^{(a)}) \\ &-\frac{1}{2} J_2 \sum_{i\alpha\beta} (b_{i,\alpha}^{\dagger(1)} b_{i,\alpha}^{\dagger(2)})(b_{i,\beta}^{(1)} b_{i,\beta}^{(2)}) \ . \end{aligned} \tag{2.4}$$

To proceed with the approximate mean-field treatment one introduces a Lagrange multiplier μ to enforce the constraint, and an in-plane bond field Q and a between-planes bond field Δ to decouple the quartic interactions in Eq. (1.1). In the mean-field approximation μ, Δ, and Q are taken to be constant in space and time. The resulting theory may be diagonalized. The manipulations are standard and are given in Appendix A. The result is a model of two species of bosons (s, for symmetric under interchange of planes, and a, for antisymmetric under interchange of planes) governed by the Lagrangian

$$\mathcal{L}_B' = \sum_{k\alpha} s_{k\alpha}^\dagger [\partial_\tau + \omega_k] s_{k\alpha} + a_{k\alpha}^\dagger [\partial_\tau + \omega_{k+P}] a_{ka} \ , \tag{2.5}$$

with

$$\omega_k = \sqrt{\mu^2 - (Q\gamma_k + \Delta)^2} \ , \tag{2.6}$$

$$\gamma_k = \frac{1}{2}(\cos k_x + \cos k_y) \ , \tag{2.7}$$

and

$$P = (\pi, \pi) \ . \tag{2.8}$$

Note that $\gamma_{k+P} = -\gamma_k$. The parameters μ, Q, and Δ are determined by the mean-field equations

$$\int \frac{d^2k}{(2\pi)^2} \frac{\mu}{\omega_k} \coth\frac{\omega_k}{2T} = 1 + 2S \ , \tag{2.9a}$$

$$\int \frac{d^2k}{(2\pi)^2} \frac{(Q\gamma_k + \Delta)\gamma_k}{\omega_k} \coth\frac{\omega_k}{2T} = Q/2J_1 \ , \tag{2.9b}$$

$$\int \frac{d^2k}{(2\pi)^2} \frac{Q\gamma_k + \Delta}{\omega_k} \coth\frac{\omega_k}{2T} = 2\Delta/J_2 \ . \tag{2.9c}$$

These equations are derived in Appendix A and imply Q, Δ, μ are real, and $\Delta, \mu > 0$. Further, one may change the sign of Q by shifting the origin of reciprocal space to $k = P$ and interchanging the labels s and a. Thus we take $Q > 0$ with no less of generality.

The integrals in Eqs. (2.9) depend on k only via γ_k; one may therefore recast them as $\int d^2k/(2\pi)^2 \to \int d\gamma N(\gamma)$ where $N(\gamma)$ is a density of states which is constant near

the band edges $\gamma=\pm 1$ and logarithmically divergent at the band center $\gamma=0$. To obtain an analytically tractable model we replace $N(\gamma)$ by $\frac{1}{2}$. The resulting equations are solved in Appendix B. At $T=0$ we find the phase diagram shown in Fig. 2. At $J_2=0$ we have two decoupled planes. As is well known[10,11,15,16] a single plane has a transition at $S=S_c\cong(\pi/2-1)/2\cong 0.28$ (the numerical expression for S_c is obtained from the mean-field calculation) between a large-S ordered state and a small-S singlet state with a gap to all spin excitations. If one increases J_2 in the ordered ($S>S_c$) phase of the one-plane model, one reaches at a $J_2\sim J_1$ another transition line, at which the ordered phase is destroyed in favor of singlets which are principally between planes. At $S=\frac{1}{2}$ the Schwinger-boson mean-field yields a second-order transition at $J_2\cong 4.48J_1$. A previous series expansion study of Eq. (1.1) by Hida[17] yielded a second-order transition at $J_2\cong 2.56J_1$ and a very recent Monte Carlo study by Sandvik and Scalapino[18] found a second-order transition at $J_2\cong(2.5\pm 0.2)J_1$.

Interesting, for $S<S_c$, we find that increasing J_2 from $J_2=0$ initially reduces the gap in the singlet phase, thus moving the system closer to order. For $S^*<S<S_c$ (with $S^*\cong 0.19$ in the mean-field calculation) the phase diagram is reentrant. We believe that the physics behind the reentrance is that a small J_2 splits the spectrum into acoustic and optic sectors, and because the optic sector involves a coupled motion of the spins in the two planes the effective spin of the model describing the low energy fluctuations is increased, promoting order, whereas at large J_2 the between-planes interaction produced singlets, favoring destruction of order.

In the disordered phase, $\mu>(Q+\Delta)$ and the excitation spectrum has a gap at all wave vectors. Two gaps that will be particularly important in what follows are ω_+ and ω_-, given by

$$\omega_+=\sqrt{\mu^2-(Q+\Delta)^2} \tag{2.10}$$

and

$$\omega_-=\sqrt{\mu^2-(Q-\Delta)^2}\ . \tag{2.11}$$

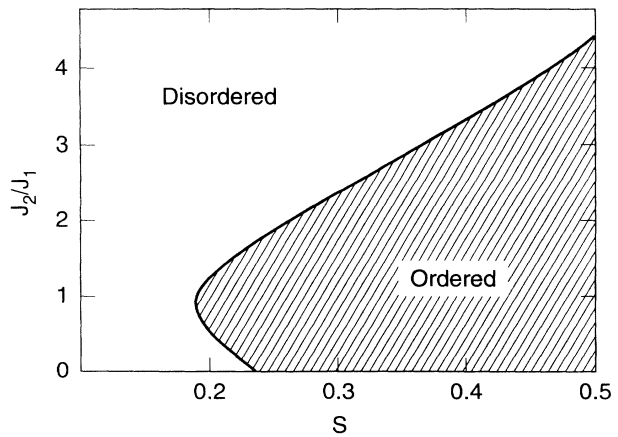

FIG. 2. $T=0$ phase diagram of Eq. (1.1) as described in Appendix B from the Schwinger-boson mean-field theory.

For the s bosons, ω_+ is the gap at $k=0$ and ω_- is the gap at $K=P$; for the a bosons, 0 and P are interchanged. We shall see that the matrix elements coupling the bosons to externally applied fields have a strong k dependence, so that measurable susceptibilities near $k=0$ differ dramatically from those near $k=P$. Both gap parameters are temperature dependent.

At the $T=0$ phase transition, ω_+ vanishes while $\omega_->0$. Near the large J_2 boundary of the ordered phase, we have $\Delta\sim Q$ and $\omega_-\sim J_1\gg\omega_+$. The s-boson mode has one low energy branch, centered at $k=0$,

$$\omega_+(k)^2=\omega_+^2+2\mu^2(1-\gamma_k)=\omega_+^2+v^2k^2\ . \tag{2.12}$$

Here we have expanded $\gamma_k=1-k^2/4$, set $Q+\Delta/\mu$ and defined $v^2=\mu^2/2$.

In the lower, reentrant branch of the phase diagram, i.e., at $T=0$, $S^*<S<S_c$, $J_2\ll J_1$, we find from Eqs. (B7) that the phase boundary is given by

$$\frac{J_2^*}{J_1}=\pi(S_c-S)+(\pi^2-8)(S-S_c)^2+\cdots\ . \tag{2.13}$$

On the phase boundary,

$$\omega_-=J_2+\cdots\ . \tag{2.14}$$

In Eqs. (2.13) and (2.14) the ellipses denote terms of order $(S_c-S)^3$, $(J_2/J_1)^3$, and higher. If we tune through the phase transition by varying J_2 we find that sufficiently deep in the ordered phase ω_- increases as $(J_2J_1)^{1/2}$ as expected from spin-wave theory,[4] while ω_- approaches ω_+ very rapidly as J_2 is decreased into the disordered phase. Indeed, within mean-field theory we find that for $J_2/J_1\le\pi(S_c-S)-(8-\pi^2/2)(S_c-S)^2$ a solution with $\omega_+\neq\omega_-$ is not possible. The sharp transition from a solution with $\omega_->\omega_+$ to one with $\omega_-=\omega_+$ is an artifact of mean-field theory. The qualitative result, that $(\omega_--\omega_+)/\omega_-$ drops rapidly as one moves into the disordered phase, is likely to be correct for this model, because the argument is that the ground state of the one-plane model in the disordered phase is a singlet with a gap of order $J_1(S_c-S)$; for J_2 less than this value the interplane coupling can only slightly perturb the singlets.

For $S=S_c$ and $J_2\ll J_1$ the s boson has two low energy branches, one centered at $k=0$ with dispersion given by Eq. (2.12) and one given by

$$\omega_-(k)^2=\omega_-^2+2\mu^2(1+\gamma_k)=\omega_-^2+v^2(k-P)^2\ . \tag{2.15}$$

Here $v=\mu/2+\cdots$ and the ellipsis indicates terms of order $(J_2/J_1)^2$.

We now consider $T>0$. In a realistic model there are no phase transitions; however, different regimes of behavior exist. In the mean-field theory, crossovers between different regimes sometimes appear as unphysical phase transitions. We are interested in properties in the disordered regime near the critical line. At the $T=0$ phase transition, ω_+ vanishes; close to it ω_+ is much smaller than J_1. For T less than the zero temperature value of ω_+, $\omega_+(T=0)$, the number of thermal excitations is negligible; the physics is of a singlet ground state

with a q-dependent gap to excitations. In the literature this is referred to as a "quantum disordered regime." In this regime the low energy spectrum only involves one linear combination of the spin excitations in the two different planes, the antisymmetric one for k near P and the symmetric one for K near 0. For $\omega_+(T=0)<T<\omega_-(T=0)$ this one linear combination becomes thermally excited. We refer to this as the "coupled-planes quantum critical regime." It only exists if $\omega_-(T=0)-\omega_+(T=0)$ is large enough. In the coupled-planes critical regime $\omega_+(T)\sim T$, but $\omega_-(T)$ takes its zero temperature value. The crossover from the quantum disordered regime to this quantum critical regime is identical to that occurring in a one-plane model. Finally, as T is increased through $\omega_-(T=0)$ the other linear combination of spin excitations also becomes excited and the two planes begin to fluctuate more or less independently. If $\omega_-(T=0)\ll J_1$, then we find in the mean-field theory that the behavior in this regime will be controlled by the $T=0$ critical point of a single plane. We refer to this regime as the "decoupled-planes critical regime." In the mean-field theory the change from the coupled-planes to the decoupled-plane regime occurs via a second-order phase transition. We expect fluctuations not included in the mean-field theory will convert this into a smooth crossover. In the decoupled-planes regime, both ω_+ and ω_- are proportional to T with the same coefficient. The left side of Fig. 3 shows the various regimes. The upper panel shows the situation near the small J_2/J_1, reentrant phase boundary of the $T=0$ phase diagram. Here region A is the quantum disordered regime, region B is the coupled-planes quantum critical regime, region C is the decoupled-planes quantum critical regime, and region D is the renormalized classical regime. The lower panel shows the situation near the large J_2/J_1 phase boundary of the $T=0$ phase diagram; here the crossover to the decoupled-planes critical regime occurs at such a large energy that it is not governed by the $T=0$ fixed point. The right-hand side of Fig. 3 shows the T dependence of ω_+ and ω_- for parameters chosen so

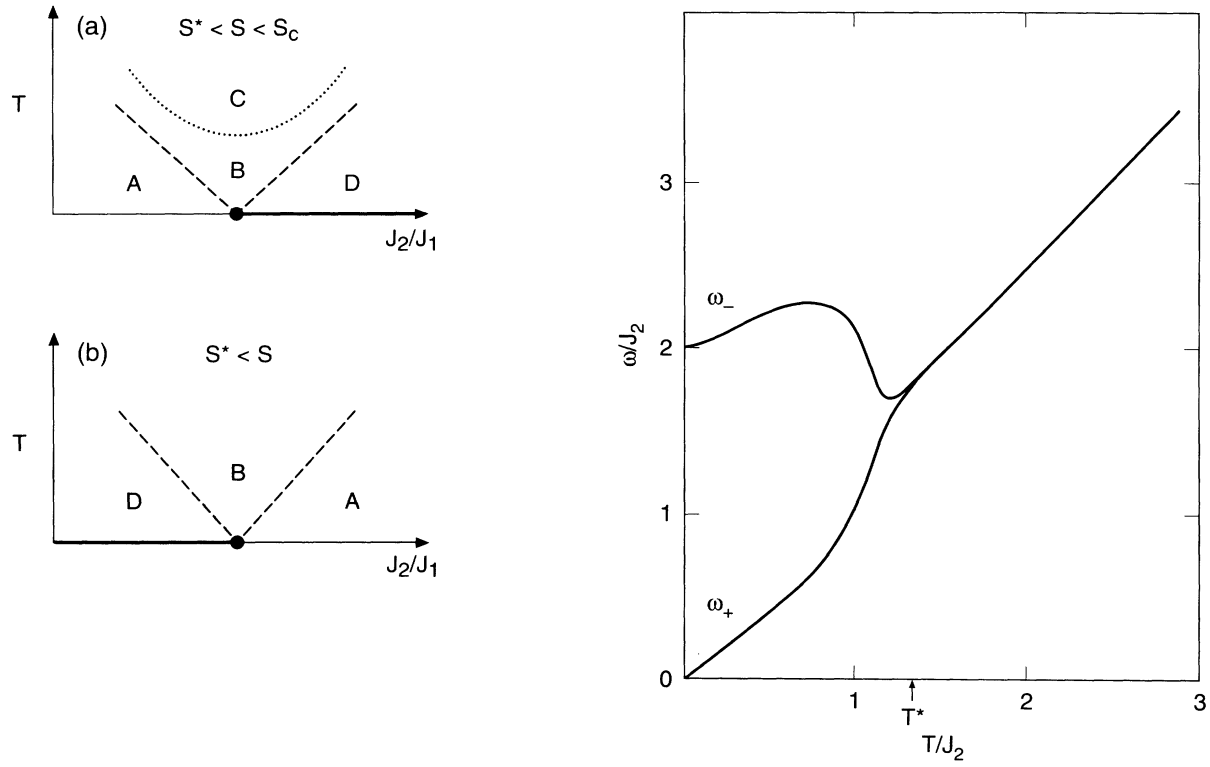

FIG. 3. (Left panel) Sketch of different regimes in T-J_2/J_1 plane. Upper panel (a), situation near small-J_2, $S^*<S<S_c$ reentrant part of phase diagram. Note that the J_2/J_1 scale has been expanded, so only the immediate vicinity of the lower transition is shown. Here the heavy dot indicates the $T=0$ critical point, the heavy line indicates the ordered phase, and the dotted and dashed lines indicate crossovers between the different regimes. A denotes the quantum disordered regime, B the coupled-planes quantum critical regime, C the decoupled-planes critical regime, and D the renormalized classical regime. Lower panel (b), situation near large-J_2 $T=0$ transition. Notation as in upper panel, but only the immediate vicinity of the upper transition is shown. Note that the decoupled-planes critical regime is absent. (Right panel) Temperature dependence (in units of J_2) of the Schwinger-boson gaps ω_+ and ω_- defined in Eqs. (2.10) and (2.11) and computed as described in Appendix B, for parameters such that at $T=0$ the model is at the phase boundary for small J_2 and S_c-S. The temperature $T^*\sim J_2$ separates the low-T coupled-planes regime from the high-T decoupled-planes regime; in the mean-field theory there is a second-order phase transition at T^*; we believe fluctuations would convert this to a smooth crossover.

that $\omega_+(T=0)=0$ (i.e., increasing temperature above the critical point shown in the upper panel of the left side of Fig. 3) and also indicates the different regimes.

III. PHYSICAL QUANTITIES

To obtain the magnetic susceptibilities we compute the linear response of the system to an externally applied magnetic field $\mathbf{h}_i^{(a)}$. The details are given in Appendix C. We find it convenient to decompose the externally applied field into parts symmetric and antisymmetric under interchange of planes, and compute the linear response to

$$\Delta H=\sum_q \frac{h_q^{(1)}-h_q^{(2)}}{2}O_q^a+\frac{h_q^{(1)}+h_q^{(2)}}{2}O_q^s \ . \tag{3.1}$$

Here O^s and O^a are operators creating spin fluctuations symmetric and antisymmetric under interchange of planes, respectively. The only nonzero susceptibilities are

$$\chi_q^{aa}(\omega)=\int_0^\infty dt e^{i(\omega+i\epsilon)t}\langle[O_q^a(t),O_{-q}^a(0)]\rangle \tag{3.2a}$$

and

$$\chi_q^{ss}(\omega)=\int_0^\infty dt e^{i(\omega+i\epsilon)t}\langle[O_q^S(t),O_{-q}^S(0)]\rangle \ . \tag{3.2b}$$

The uniform susceptibility (written as a susceptibility per spin and *not* as a susceptibility per unit cell) is

$$\chi(T)=\lim_{q\to 0}\chi_q^{ss}(\omega=0)=\frac{1}{4T}\sum_k \sinh^{-2}\left[\frac{\omega_k}{2T}\right] \ . \tag{3.3}$$

We note that in the approximation of Sec. II and the Appendixes, namely,

$$\frac{kdk}{2\pi}=N(\gamma)d\gamma=\frac{\omega d\omega}{2} \ , \tag{3.4}$$

Eq. (3.3) becomes

$$\chi(T)=2T\left[\int_{\omega_+/2T}^\infty \frac{dxx}{\sinh^2(x)}+\int_{\omega_-/2T}^\infty \frac{dxx}{\sinh^2(x)}\right] \ . \tag{3.5}$$

From Eq. (3.5) we see that in the coupled-planes quantum disordered regime $\omega_+(T=0)\gg T$, $\chi(T)\sim\omega_+ e^{-\omega_+/T}$; this is a factor of 2 smaller than would be found for a single plane in the disordered regime with the same gap. In the coupled-planes critical regime $\omega_+(T=0)\ll T \ll\omega_-(T=0)$, $\chi(T)\sim T$, and in the decoupled-planes critical regime $T\ll\omega_-(T=0)$, we also have $\chi(T)\sim T$ but with a coefficient larger by a factor of 2. This behavior is easy to understand: in the coupled-planes regime one of the two spin degrees of freedom per unit cell is frozen out; in the decoupled-planes region both are free to fluctuate.

Next we consider $\chi''(q,\omega)$ for $q=P$. From the results of Eqs. (3.2) we find, for $\omega>0$.

$$\chi_P^{aa''}(\omega,T)=\frac{\pi}{\omega}\coth(\omega/4T)[\Theta(\omega-2\omega_-)+\Theta(\omega-2\omega_+)] \ , \tag{3.6}$$

$$\chi_P^{ss''}(\omega,T)=\frac{2\pi}{\omega}\{\Theta(\omega-(\omega_++\omega_-))[1+b((\omega^2-\omega_+^2+\omega_-^2)/2\omega)+b((\omega^2+\omega_+^2-\omega_-^2)/2\omega)]$$
$$+\Theta(\omega_--\omega_+-\omega)[b((\omega_-^2-\omega_+^2-\omega^2)/2\omega)-b((\omega_-^2-\omega_+^2+\omega^2)/2\omega)]\} \ . \tag{3.7}$$

These formulas are plotted in Fig. 4 for the parameters used to construct Fig. 3. The sharp onset at $T=0$ is an unphysical feature of the dynamics in the mean-field theory, which is removed when fluctuations are included.[11,19] A related peculiarity of the mean-field theory is that $\chi'(q,\omega=0)$ decays as $1/q$ for q near P. We believe that despite the obvious artificialities the mean-field expressions give some reliable information about the spin excitations of the model, as in the case of the one-plane Heisenberg model.[15] In particular, we believe that the location of the peaks and their relative magnitudes and temperature dependences give a reasonable representation of the location, relative magnitude, and temperature dependence of the peaks in the appropriate susceptibilities of the model. We see that from Eqs. (3.6) and (3.7) and Fig. 4 that at low T the important energy scale for $\chi_P^{aa''}$ is $2\omega_+$ while for $\chi_P^{ss''}$ it is $\omega_++\omega_-$. Everywhere in the disordered phase the difference between these energies is less than J_2. It is also clear that until the temperature becomes comparable to the scale T^* at which the crossover from the coupled-planes to the decoupled-planes critical regime occurs, $\chi_P^{aa''}\gg\chi_P^{ss''}$, and that $\chi_P^{ss''}$ is confined mostly to high frequencies, of order $2J_2$. For this reason we suspect that the neutron scattering data,[4,5] which have not observed any $\chi_P^{ss''}$ component for $\omega<40$ meV, do not set a stringent limit on J_2, although they suggest that it is greater than 20 meV.

We now turn to the relaxation rates. Details of the computations may be found in Appendix C. We begin with that of yttrium, $1/{}^YT_1T$, which is found to be

$$\frac{1}{{}^YT_1T}=2\pi D^2\lim_{\omega\to 0}\frac{1}{\omega}\sum_q |g(q)|^2\chi_q^{ss''}(\omega) \ . \tag{3.8}$$

The form factor g is equal to 4 for q near 0 and to $(q-P)^2$ for q near P; a more precise formula is given in Eq. (C15).

Using Eqs. (3.4) and (C15) we find

$$\frac{1}{{}^YT_1T}=8\pi D^2T^2\left[\int_{\omega_+(T)/2T}^\infty \frac{dxx^2}{\sinh^2(x)}+\int_{\omega_-(T)/2T}^\infty \frac{dxx^2}{\sinh^2(x)}\right] \ . \tag{3.9}$$

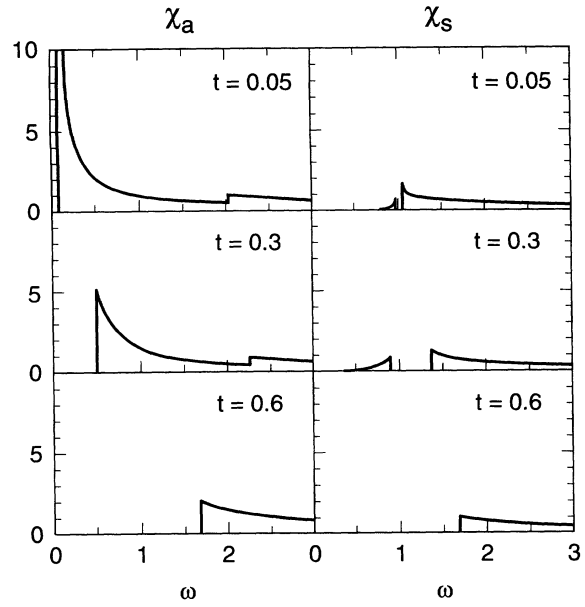

FIG. 4. Frequency dependence of antisymmetric and symmetric susceptibilities calculated from mean-field theory for several different temperatures.

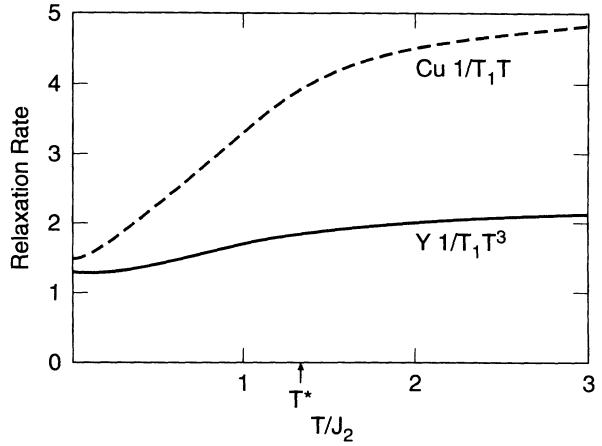

FIG. 5. Temperature dependence of copper and yttrium relaxation rates calculated from mean-field theory for parameters used in constructing Fig. 3. Note that the yttrium relaxation rate has been divided by two additional powers of T. The temperature T^* at which the model crosses over from the decoupled-planes to the coupled-planes critical regimes is indicated.

In the mean-field approximation to both the coupled-planes and the decoupled-planes critical regimes, the yttrium rate $1/^{Y}T_1T \sim T^2$, and so it vanishes faster than the static susceptibility, while in the low-T limit $1/^{Y}T_1T \sim e^{-\omega_+/T}$ is proportional to the uniform susceptibility. Note that the ratio of $1/^{Y}T_1T$ to χ^2 is the same in the coupled-planes critical regime as it is in the decoupled-planes critical regime. There are two compensating effects at work: in the coupled-planes regime there is only one spin mode at small q (instead of the two that occur in a model of two uncoupled planes) but in this mode the eight spins add coherently to the yttrium relaxation rate, whereas in the decoupled-planes regime there are twice as many spin excitations (so one would naively expect the rate to be 4 times as large) but the two planes add incoherently (reducing the rate by a factor of 2). $1/^{Y}T_1T$ is divided by two additional powers of T and plotted in Fig. 5 for the parameters used to construct Fig. 3.

We now consider the oxygen rate. This has one contribution from the small-q fluctuations and one from fluctuations with q near P. The latter is suppressed by a form factor because each oxygen sits symmetrically between two copper sites, and so a perfectly antiferromagnetic fluctuation would cancel on the oxygen site.[2] The result, derived in Eq. (C17), is

$$\frac{1}{^{O}T_1T} = \frac{C^2}{4} \lim_{\omega\to 0} \frac{1}{\omega} \sum_q |f(q)|^2 [\chi_q^{ss''}(\omega) + \chi_q^{aa''}(\omega)] \, . \tag{3.10}$$

This is precisely the usual result.[2] Again using the approximation of Eq. (3.4), we get

$$\frac{1}{^{O}T_1T} = C^2(2T)^2 \left[\int_{\omega_+(T)/2T}^{\infty} dx \frac{2x^2 - (\omega_+/2T)^2}{\sinh^2(x)} + \int_{\omega_-(T)/2T}^{\infty} dx \frac{6x^2 - 2(\omega_+/2T)^2 - (\omega_-/2T)^2}{\sinh^2(x)} \right] . \tag{3.11}$$

In contrast to the yttrium, where the variation was by a factor of 2, here the coefficient of the T^2 term varies by a factor of 4 between the coupled- and decoupled-planes critical regimes.

In the mean-field theory the oxygen rate varies as T^2 in the critical regime. We shall see in the next section that in the more physically reasonable scaling analysis the antiferromagnetic spin fluctuations lead to an oxygen relaxation rate proportional to T in the critical regime.

We now turn to the copper rate, which is given by

$$\frac{1}{^{Cu}T_1T} = \frac{1}{4} \lim_{\omega\to 0} \frac{1}{\omega} \sum_q [A - 4B\gamma(q)]^2 \times [\chi^{ss''}(q,\omega)\chi^{aa''}(q,\omega)] \, . \tag{3.12}$$

Again this may be evaluated, giving

$$\frac{1}{{}^{Cu}T_1T}=\frac{(A-4B)^2}{4}\left[\int_{\omega_+(T)/2T}^{\infty}dx/\sinh^2(x)+3\int_{\omega_-(T)/2T}^{\infty}dx/\sinh^2(x)\right]. \tag{3.13}$$

This also is plotted in Fig. 5 for the parameters used in Fig. 3. Note there is a factor-of-4 change from the coupled-planes critical regime to the decoupled-planes critical regime. Note that in the critical regime the Cu relaxation rate is T independent. Again, this is due to the artificiality of the Schwinger-boson mean-field theory. The scaling analysis predicts a $1/T$ behavior.[11]

IV. SCALING ANALYSIS

The mean-field analysis of the previous sections is known[11,19,20] to give incorrect results for dynamical susceptibilities for the single-plane Heisenberg model at finite spin degeneracy N. A scaling theory which corrects these discrepancies has been developed.[10,11] In this section we extend the scaling theory to the coupled-planes system of interest here, and also construct a universal amplitude ratio for the NMR T_1 and T_2 relaxation times.

In the scaling theory of the one-plane model the important parameters for the physics on the disordered side of the phase boundary are the spin-wave velocity v, the $T=0$ gap to spin-1 excitations, Δ, the quasiparticle residue of the lowest-lying $S=1$ excitation at $T=0$, A_{QP}, and the temperature T. Low energy physical quantities are universal functions of these parameters. Further, one must distinguish the "quantum disordered" $T\ll\Delta$ regime from the "quantum critical" $T\gg\Delta$ regime.

We now extend the theory to two coupled planes. We expect on general grounds and showed explicitly using the mean-field theory that the between-planes coupling J_2 splits the spin excitation spectrum into acoustic and optic branches. The minimum gap to optic excitations, Δ_o, is nonzero for $J_2>0$; the acoustic excitations acquire a gap Δ_a in the disordered phase. In the mean-field treatment of the previous section, $\Delta_a=2\omega_+$ while $\Delta_o=\omega_++\omega_-$. We found that on the phase boundary $\Delta_o\sim J_2$ while $\Delta_a=0$. As one moves into the disordered phase, Δ_a rapidly approaches Δ_o. Deep in the ordered phase, for small J_2, $\Delta_o\sim\sqrt{J_1J_1}$ in agreement with spin-wave theory.[4]

As we tune the system through the order-disorder transition, Δ_o remains nonzero, so the optic fluctuations are irrelevant in the renormalization group sense. Within the mean-field approximation the transition is thus one in which the Heisenberg order vanishes and a single twofold-degenerate spin-wave mode of velocity v_a acquires a gap Δ_a. The usual universality arguments then imply that the transition is in the previously considered universality class, and that at $\omega,T\ll\Delta_o$ the physical quantities are given by the previously calculated universal functions[11] evaluated at arguments v_a and T/Δ_a. We refer to this $\omega,T\ll\Delta_a$ regime as the "coupled-planes" regime, and distinguish the $T\ll\Delta_a$ "*coupled-planes disordered regime*" from the $T\gg\Delta_a$ "*coupled-planes critical regime.*" Of course, if $(\Delta_o-\Delta_a)/\Delta_o$ is too small the coupled-planes critical regime may not exist.

There is one subtlety in the analysis of the coupled-planes regime: The universal forms give susceptibilities in units of emu/area. A unit cell contains two Cu atoms (one in each plane); the susceptibilities are evenly divided between the two planes, and thus the susceptibilities per Cu are one-half of the one-plane values. Further, because the Cu and O nuclei of interest for high-T_c NMR experiments sit in one CuO_2 plane, the hyperfine coupling of the Cu or O nucleus to the surviving spin degree of freedom is half as large as in a single-plane model, and so the Cu and O relaxation rates, which go as the square of the hyperfine coupling constant, will be one-quarter of the usual size. The yttrium nucleus, however, sits between two planes and over the center of a plaquette of four Cu nuclei. In the coupled-planes regime the hyperfine coupling per moment is half the expected value, but the eight nearest-neighbor spins add coherently, and so the yttrium NMR rate is only one-half of the expected value. These factors were explicitly derived in the mean-field analysis of the previous section; we have given a qualitative argument here.

As one increases the temperature from zero in the disordered phase one passes first through the coupled-planes disordered regime and then, if $(\Delta_o-\Delta_a)/\Delta_o$ is sufficiently large, through the coupled-planes critical regime. As one continues to increase the temperature it becomes comparable to the optic mode energy Δ_o and the bilayers become uncorrelated. If Δ_o is sufficiently small, i.e., if $J_2\ll J_1$, then at $T>\Delta_o$ the physics will still be controlled by a $T=0$ critical point. We showed using the mean-field theory that in this regime each plane fluctuates independently and is in the quantum critical regime of a one-plane model. We believe this conclusion survives beyond mean-field theory. We refer to the regime $T>\Delta_o$ as the "*decoupled-planes critical regime.*" It is probable that one could extend the calculation of Ref. 11 to incorporate fluctuations into our mean-field analysis of the crossover between the coupled- and decoupled-planes regimes, but we have not attempted this. Instead, we consider the uniform susceptibility and NMR rate in each regime separately. The scaling properties of the single-plane transition have recently been elegantly derived and discussed.[11] We summarize, as briefly as possible, the results we will need and their extension to the two-plane system.

The correlation length ξ is a universal function of T and Δ,

$$\xi=\frac{\hbar v}{k_BT}X(k_BT/\Delta), \tag{4.1}$$

where $X(y)$ a universal function which tends to a number very nearly unity (1.03 in a large-N expansion with terms of order 1 and $1/N$ included and N set equal to 3) as y tends to infinity (so $\xi\sim\hbar v/k_BT$ for $T\gg\Delta$) and to y as y tends to zero (so ξ tends to $\hbar v/\Delta$ for small T). Note that for $J_2\ll J_1$, v is essentially the same for acoustic and optic modes, so that this relation is valid in both coupled- and decoupled-planes regimes.

The divergent part of the order parameter susceptibility, χ_{AF}, may be written

$$\chi_{AF}(q,\omega;T)=\chi_{AF}\xi^{2-\eta}\phi_{AF}(q\xi,\omega\xi/v;T/\Delta) . \quad (4.2)$$

Here χ_{AF} contains the dimensions and ϕ_{AF} is a universal function. We have introduced the exponent η for completeness even though for the transition in question it is very nearly zero.[11,21] In the coupled-planes regime we should interpret this as a susceptibility per unit area; in the decoupled-planes regime as a susceptibility per area per plane. χ_{AF} is a critical amplitude; its value is not universal but from it and other measurable quantities universal amplitude ratios may be constructed. In particular, $\chi_{AF}=A_{QP}/v^2$ where A_{QP} is the quasiparticle residue of the lowest-lying $S=1$ excitation in the disordered phase at $T=0$ and we have made explicit the factors of the velocity which were set to unity in Ref. 11.

The uniform susceptibility has also a scaling form; here even the dimensional prefactor is known.[11] The susceptibility in units of emu per area is

$$\chi_u(q,\omega;T)=\frac{g^2\mu_B^2}{\hbar v\xi}\phi_u(k_BT/\Delta)\frac{(D_s/\xi)(q\xi)^2}{-i\omega\xi+D_s/\xi(q\xi)^2} . \quad (4.3)$$

Here g is the electron g factor and μ_B is the Bohr magneton. Again this is a susceptibility per unit area in the coupled-planes regime and a susceptibility per area per plane in the decoupled-planes regime. D_s is the spin diffusion coefficient; it has a dependence on T and q which we have suppressed here. ϕ_u is a universal function which tends to a constant as y tends to infinity and vanishes rapidly as y tends to zero. It is usually assumed that the quantity $g\mu_B$ may be taken to have free electron values because in the nonlinear σ-model treatment of the critical point it is not renormalized from its bare value; however, this assumption has not been proven for more general models.

We shall be most interested in applying this formula in the critical regime $T\gg\Delta$; we therefore proceed to estimate D_s in this regime. We argue that for the modes relevant to NMR experiments,

$$D_s=D_s^0v^2\frac{\hbar\ln^{1/2}(1/q)}{k_BT} . \quad (4.4)$$

Here D_s^0 is a number, presumably of order unity. The factor of $1/T$ arises as follows. For excitations of velocity v and scattering rate Γ, $D_s\sim v^2/\Gamma$. Further, conventional dynamic scaling suggests that modes at scales shorter than the correlation length are weakly damped, while those at longer scales are overdamped, implying that the scattering rate for spin excitations is proportional to T. The factor of $\ln^{1/2}$ comes from the breakdown of hydrodynamics in two spatial dimensions.[22]

We are now able to discuss relaxation rates. We begin with the yttrium rate. We saw in the previous section that the yttrium nucleus is coupled only to fluctuations of the uniform magnetization. By comparing the notations of this and the previous section we see that in the coupled-planes regime the coupling constant is $4Da^2/\mu_Bg$ (recall that there are eight Cu neighbors but that the spin density is evenly divided between the two planes). Calculating the relaxation rate in the usual way give

$$\frac{\hbar}{{}^YT_1k_BT}=\frac{16D^2a^4}{\hbar^3D_s^0v^3\xi}\frac{k_BT}{\pi}\ln^{1/2}(1/qa) . \quad (4.5)$$

Recall that ϕ_u refers to two planes; normalizing per plane restores the factor of 32 from (3.9). A power of $\ln^1$ was obtained previously by Chakravarty and Orbach in a calculation of relaxation in an ordered magnet;[20] the different power comes because they did not consider the corrections to hydrodynamics. The logarithm will be cut off at some scale by a three-dimensional coupling J_{3D} and is presumably not important in practice. The important result is that in the quantum disordered regime both D_s and ξ go as $1/T$, so the yttrium relaxation rate in this model is proportional to T^2 up to logarithms, as was found in the mean-field theory of the previous section. In the decoupled-planes critical regime the calculation is identical except that we must add two contributions, one from each plane. For each contribution the coupling constant is $4Da^2/\mu_Bg$ and we must neglect interplanar correlations. The result is a factor-of-2 increase in the coefficient of the T^2 term, as was found in mean-field theory.

We now consider the oxygen relaxation rate. This has one contribution from the small-q fluctuations which may be evaluated as we did for yttrium and which will be seen to be subdominant, and another contribution from the antiferromagnetic fluctuations, which we evaluate. The coupling constant connecting the oxygen nucleus to an antiferromagnetic fluctuation in a given plane of wave vector q (measured from P) may be written $C_{AF}a^2f(qa)$ where C_{AF} is *a priori* not the same as the coupling constant C introduced before. Symmetry implies that $f(x)\sim x^2$ at small x. COmbining this with Eq. (4.2) for χ_{AF} gives, in the coupled-planes regime,

$$\frac{\hbar}{{}^OT_1k_BT}=\frac{1}{4}\frac{C_{AF}^2a^3}{\hbar v}\frac{\chi_{AF}}{\mu_B^2}(\xi/a)^{-(1+\eta)}\phi_0(T/\Delta_a) . \quad (4.6)$$

Here $\phi_0(z)$ is a universal function obtained by integrating $\lim_{y\to0}x^2\phi''_{AF}(x,y;z)/y$ over x. We have assumed the integral converges, in the spin-only model this is reasonable because at momentum scales larger than the inverse correlation length the model goes over to spin-wave theory and the integrals there converge. In a more general model the issue of convergence is less clear. Thus the oxygen relaxation rate in this model scales at $T^{1+\eta}$ with a nonuniversal prefactor involving both the hyperfine coupling C_{AF} and the amplitude χ_{AF}. The oxygen relaxation rate scales differently from the yttrium because the oxygen is coupled (albeit weakly) to the antiferromagnetic fluctuations, while the yttrium is not. As we have previously argued, the constant C_{AF} is larger by a factor of 2 in the decoupled-planes regime than it is in the coupled-planes regime, leading to a factor-of-4 change in the relaxation rate.

We finally consider the copper. This is coupled to the spins by a matrix element $A_{\rm AF}a^2/\mu_B$. The relaxation rate in the coupled-planes regime is

$$\frac{\hbar}{{}^{\rm Cu}T_1 k_B T}=\frac{A_{\rm AF}^2 a^3}{4\hbar\mu}\frac{\chi_{\rm AF}}{\mu_B^2}(\xi/a)^{1-\eta}\phi_{\rm Cu}(T/\Delta)\ . \quad (4.7)$$

Thus the Cu relaxation rate $1/T_1T$ in this model scales at $T^{\eta-1}$ times a nonuniversal prefactor involving both the hyperfine coupling and the amplitude $\chi_{\rm AF}$. The formula (4.7) has been previously given.[11] The same factor-of-4 change in the coefficient of the leading T-dependent term between the coupled-planes and decoupled-planes regimes that occurred for the oxygen relaxation rate occurs for the copper.

The T_1 relaxation rate is determined by the imaginary part of χ. The T_2 rate measures the real part of χ. Specifically, in circumstances relevant to experiments on high-T_c materials,[23]

$$\left[\frac{1}{T_2}\right]^2=n_m\sum_q[A_{\rm AF}\chi'(q,\omega=0)]^2\ , \quad (4.8)$$

where n_m is the density of NMR nuclei. Substituting the scaling ansatz and integrating gives

$$\frac{\hbar}{T_2}=n_m^{1/2}\frac{A_{\rm AF}^2 a^3\chi_{\rm AF}}{\mu_B^2}(\xi/a)^{1-\eta}\phi_{T2}(T/\Delta)\ . \quad (4.9)$$

By combining Eqs. (4.7) and (4.9) we see that apart from the factor $n_m^{1/2}$ and the velocity v, the ratio of T_2 to T_1T is universal, and indeed takes the same value in the coupled-planes and decoupled-planes critical regimes. Note, however, that in the coupled-planes regime the contribution of the optic excitations to $1/T_2$ will be large (of order $1/\Delta_o$). The contribution of the acoustic sector is of order $1/\Delta_a$. Thus $1/T_2$ will attain its universal value in the coupled-planes regime only if $(T,\Delta_a)\ll\Delta_o$.

Sokol and Pines[9] have previously made the interesting observation that the observed T independence of T_2/T_1T in $YBa_2Cu_3O_{6.6}$ for $T>150$ K suggests that the magnetic dynamics in this material is controlled by the $z=1$ critical point considered here. We see that the magnitude provides information about the velocity v and that this must be consistent with the uniform susceptibility.

V. CONCLUSION

We have studied some aspects of the $T=0$ magnetic-nonmagnetic transition occurring in a model of two antiferromagnetically coupled planes of antiferromagnetically correlated spins. This model is defined in Eq. (1.1) and depicted in Fig. 1. The two dimensionless parameters are J_2/J_1 (the ratio of the between-planes coupling J_2 to the in-plane coupling J_1) and S, the magnitude of the spin in one plane. The important dimensional parameter is the spin-wave velocity v. The phase diagram at $T=0$ in the J_2/J_1-S plane is shown in Fig. 2. For a single plane (i.e., $J_2=0$), decreasing S through a critical value S_c causes a phase transition between a magnetically ordered phase and a singlet phase with a gap to spin excitations. Some properties of this transition were determined by Chakravarty, Halperin, and Nelson[10] and it was analyzed in detail by Sachdev and co-workers.[11] For the coupled-planes system we found using a Schwinger-boson mean-field theory that a large value of the interplanar coupling J_2 destroys the magnetism even for $S>S_c$ (because it favors binding of nearest-neighbor spins on different planes into singlets), while a small J_2 promotes order by increasing the effective size of the spin in a unit cell. The interplay of these two different sorts of physics leads to the reentrant phase diagram shown in Fig. 2. This phase diagram differs in an important respect from our previous interpretation of the data on spin susceptibilities of $La_{2-x}Sr_xCuO_4$ and $YBa_2Cu_3O_{6.6}$.[7] In both compounds it is clear that doping destroys the magnetism. In $La_{2-x}Sr_xCuO_4$ interplane coupling is negligible and at least the Cu relaxation rate and single-crystal susceptibility data show no clear evidence of a singlet phase with a gap to excitations (although some susceptibility and Knight shift data have been so interpreted.[9,11]) On the other hand, in $YBa_2Cu_3O_{7-\delta}$ it is clear that the nearest-neighbor CuO_2 planes are coupled by an interaction at least of order 300 K, and "spin-gap" effects are very easily observed in susceptibilities and relaxation rates for $0.1<\delta<0.5$. Thus it appears that in the real materials a presumably modest between-planes coupling promotes "spin-gap" behavior, and therefore that the spin-only model is missing some essential feature of the physics, most likely related to the presence of mobile holes.

Although it is not completely realistic, the coupled-planes model might capture some aspects of the physics of $YBa_2Cu_3O_{6.6}$ and $YBa_2Cu_4O_8$. We therefore calculated the predictions of the model for the temperature and frequency dependence of the susceptibilities measured in NMR and neutron scattering using the Schwinger-boson mean-field method and a scaling analysis. We studied parameters such that the model has no long-range order at $T=0$. The behavior in the disordered phase of a single plane of Heisenberg spins is understood.[11,16] In the single-phase case, the important parameter is the $T=0$ gap to spin-one excitations, Δ. The spin-one excitations are essentially spin waves with a gap. There are several regimes of temperature. For $T\ll\Delta$ the number of thermal spin excitations is negligible; the static spin susceptibility at $q=0$ and the dissipative part of the dynamic susceptibility at all q and at $\omega\ll\Delta$ have an activated temperature dependence $\sim e^{-\Delta/T}$. This regime is referred to as the "quantum disordered regime." If the microscopic exchange constant $J\gg\Delta$, then for $\Delta\ll T\ll J$ another regime exists in which the physics is dominated by the $T=0$ critical point but the gap is not important. In this regime the static uniform susceptibility is proportional to T and the antiferromagnetic correlation length grows as $1/T$. The regime is referred to as the "quantum critical regime."

In the two-plane model of interest here the between-planes coupling J_2 splits the spin excitation spectrum into acoustic and optic modes. There are two important scales: Δ_a, the $T=0$ gap to acoustic excitations, and Δ_o, the $T=0$ gap to optic excitations. Both gaps are nonzero

in the disordered phase. At the antiferromagnetic-singlet transition Δ_a vanishes while Δ_o remains nonzero. At the transition we found from the mean-field theory that $\Delta_o = J_2$. As one moves deeper into the disordered phase, $(\Delta_o - \Delta_a)/\Delta_o$ decreases rapidly. If one is sufficiently close to the phase boundary, so that $0 < \Delta_a \ll \Delta_o \ll J_1$, there are three regimes. These are depicted in Fig. 6. For $(T,\omega) \ll \Delta_o$ the optic mode of the two-plane system is frozen out and the physics is dominated by the acoustic mode of the two-plane system. We refer to this as the "coupled-planes regime." For $(T,\omega) \ll \Delta_a$ even the acoustic mode is frozen out. This is the "coupled-planes disordered regime." For $\Delta_a \ll T \ll \Delta_o$ the acoustic mode is thermally activated and the system is in the "coupled-planes quantum critical regime." Finally, for $\Delta_o \ll T$ the coupling between the planes become negligible and the planes fluctuate independently. This is the "decoupled planes regime." If $\Delta_o \ll T \ll J$, then we argued that the spin dynamics in each plane is separately given by the quantum critical behavior of a one-plane model. Of course, if $(\Delta_o - \Delta_a)/\Delta_o$ is too small, the coupled-planes critical regime does not exist, while if Δ_o/J_1 is too large, the physics in the decoupled-planes regime will not be controlled by a $T=0$ critical point.

We now summarize the results we obtained in Secs. III and IV for the temperature and frequency dependences of the NMR rates and susceptibilities. We found that the difference $\Delta_o - \Delta_a < J_2$ everywhere in the disordered phase and that the contribution from the optic modes near the antiferromagnetic point was rather small and only weakly temperature dependent if $\Delta_o \gg \Delta_a$. The uniform susceptibility $\chi(T)$ is activated in the coupled-planes disordered regime; in the coupled-planes critical regime $\chi(T) = 0.5ET$ (here E is a number) and in the decoupled-planes critical regime $\chi(T) = ET$. The factor-of-2 change in the coefficient of T between the coupled- and decoupled-planes regimes was derived explicitly from the Schwinger-boson mean-field theory. The physical origin, we believe, is that in the coupled-planes regime one of the two spin modes at each k (namely, the optic mode) is frozen out and does not contribute to χ, whereas in the decoupled-planes regime both modes contribute.

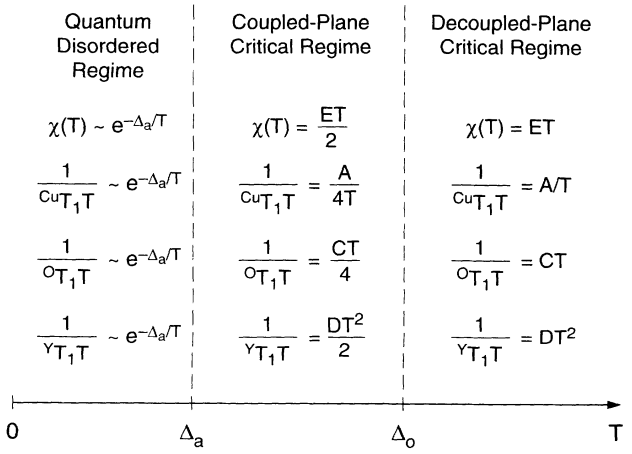

FIG. 6. Different regimes of behavior of scaling theory and temperature dependence of relaxation rates in each regime.

The T dependences of the nuclear relaxation rates are more subtle. They are summarized in Fig. 6. We consider first the copper and oxygen rates. In the quantum disordered regime all rates are activated. In the coupled-planes critical regime the Cu rate $1/T_1T = 0.25A/T$ while the oxygen rate is given by $0.25CT$. Here we have set the exponent η, which is in practice very small[21] to zero. A and C are constants. In the decoupled-planes critical regime the formulas are the same except that the number 0.25 becomes 1. The factor-of-4 change in the coefficient of the leading T dependence of the Cu and O rates between the coupled-planes and decoupled-planes critical regimes was derived from the mean-field theory. We believe that the physical origin is that in the coupled-planes regime only the acoustic mode contributes to relaxation rates. In this mode the spin fluctuation is evenly divided between the two planes; the hyperfine coupling constant connecting a Cu or O nucleus in a given plane to the spin fluctuation is thus half of what it would be in a one-plane theory, and the rate goes as the square of the hyperfine coupling. The factor-of-4 variation has an interesting implication for estimates of the relative strengths of the antiferromagnetic spin fluctuations in different materials. Authors (including us) who had considered the question previously argued that because the Cu relaxation rate in $YBa_2Cu_3O_{7-\delta}$ was smaller than in $La_{2-x}Sr_xCuO_4$, while the hyperfine couplings were approximately the same, the spin fluctuations must be weaker in the former material. We see now that until one knows whether $YBa_2Cu_3O_{7-\delta}$ is in the coupled-planes or decoupled-planes regime one cannot meaningfully compare the magnitudes of the relaxation rates to those of La_2CuO_4.

The yttrium relaxation rate behaves slightly differently, because the yttrium nucleus is coupled to a symmetric combination of Cu nuclei in the two planes. In the disordered regime the yttrium rate is activated, in the coupled-planes critical regime it goes as $0.5DT^2$, and in the decoupled-planes critical regime it goes as DT^2. The yttrium rate changes only by a factor of 2 between the coupled-planes and decoupled-planes critical regimes because in the coupled-planes regime the spins in different planes move coherently while in the decoupled-planes regime the spins move incoherently. The difference between coherent and incoherent addition of spin fluctuations produces a factor of 2 which partially compensates for the factor of 4 discussed previously.

We now consider the implications of our results for experiments on $YBa_2Cu_3O_{6.6}$ and $YBa_2Cu_4O_8$. Below $T = T^* \sim 150$ K all of the relaxation rates including the Cu $1/T_1T$ drop as T is decreased. We believe that this can only occur if the physics below $T \sim 150$ K is dominated by thermal excitations above a $T=0$ singlet state with a gap to spin excitations. In a spin-only model such as that considered here one would model this by choosing a value of spin S such that the system was near to, but on the disordered side of, the phase boundary in Fig. 2. Further, the value of T^* implies that $\Delta_a \sim 150$ K.

We must next consider the value of the interplanar coupling J_2. The experimental evidence is not conclusive. Only the acoustic excitation of the two-plane system has been observed via neutron scattering in any member of the YBa_2 family of high-T_c materials.[4,5] The main effort has been at energies less than 40 meV and temperatures less than 150 K. This would suggest that in the metallic YBa materials, $\Delta_o \geq 40$ meV. NMR measurements on $YBa_2Cu_3O_8$ provide more information. The Cu T_1 has been found to obey very well the Curie law $1/T_1T \sim 1/T$ for 200 K $< T <$ 700 K.[24] This implies that the temperature scale at which the bilayers become decoupled in this material is less than 200 K or greater than 700 K. We believe a bilayer coupling greater than 700 K would be very hard to justify on theoretical grounds. The argument is that the in-plane $J \sim 1500$ K, while $J_2 \ll J_1$ because band structure[25] and photoemission[26] results imply that the between-planes hybridization is much less than the in-plane hybridization, and the exchange energy scales as a high power of the hybridization. However, a bilayer coupling much less than 200 K may not be consistent with the neutron data. From the mean-field theory we found $\Delta_o \leq J_2 + \Delta_a$; our estimate $\Delta_a \sim 150$ K then implies $\Delta_o \leq 350$ K if $J_2 < 200$ K. Thus presently available data provide somewhat contradictory answers to the question whether $YBa_2Cu_4O_8$ is in the coupled-planes or decoupled-planes regime for 200 K $\leq T \leq$ 700 K. In what follows we consider both possibilities.

We now turn to a more quantitative discussion. Sokol and Pines have proposed that the magnetic dynamics of underdoped high-T_c materials are determined by the critical point discussed here, and their discussion has been amplified and extended by Barzykin *et al.*[9] They do not consider the bilayer coupling. They propose that these materials are in the quantum critical regime for $T \geq 150$ K and in the quantum disordered regime for $T \leq 150$ K. The essential piece of evidence they cite in favor of their proposal is the observed approximate T independence of the ratio T_1T/T_2 for 150 K $\leq T \leq$ 300 K. The observed[27] magnitude of this ratio is approximately one-half of the value observed[28] in La_2CuO_4 and calculated[29] for the $S = \frac{1}{2}$ Heisenberg model with $J = 0.13$ eV. The density n_m of ^{63}Cu NMR ions is the same in the La-Sr and YBa materials, and so we conclude from Eq. (4.9) that if the magnetic dynamics of $YBa_2Cu_3O_{6.6}$ and $YBa_2Cu_4O_8$ are well described by the universal scaling forms in either the coupled-planes or the decoupled-planes regimes, then the appropriate spin-wave velocity v is about one half of the 0.8 eV Å appropriate for La_2CuO_4,[30] i.e.,

$$v_{YBa} = 0.4 \text{ [eV Å]} . \tag{5.1}$$

The value of v makes a prediction for the magnitude of the correlation length. From Eq. (4.1) we find $\xi/a = 4$ at $T = 300$ K and $\xi/a = 6$ at $T = 200$ K; below this temperature the crossover to the quantum disordered regime presumably means that the T dependence of the correlation length becomes much weaker. These lengths are rather larger than observed in neutron scattering experiments.[3,4]

These considerations also have an implication for the Cu T_1 relaxation rate. In the quantum critical regime, the theoretical result for the Cu relaxation rate is $1/T_1T = A/T$. The coefficient $A \sim A_{QP}/v^2$,[11] where A_{QP} is the quasiparticle residue of the lowest-lying $S = 1$ state above the gap at $T = 0$. It may in principle be determined from neutron scattering measurements at low T. The coefficient A also depends on hyperfine couplings [which have been claimed to be the same in La_2CuO_4 as in $YBa_2Cu_3O_{6.6}$ and $YBa_2Cu_4O_8$ (Refs. 2, 31)] and on whether the material is in the coupled-planes or decoupled-planes regimes. In the absence of a measurement of A_{QP} one cannot definitely calculate the Cu relaxation rate; however, it is interesting to attempt to estimate it. We first argue as follows: La_2CuO_4 has been claimed to be in the quantum critical regime for $T > 600$ K;[9,11,28] further, at these temperatures the Cu T_1 has only a weak doping dependence, implying that the combination A_{QP}/v^2 depends only weakly on doping. If this is correct, then we would expect that if $YBa_2Cu_3O_{6.6}$ and $YBa_2Cu_4O_8$ were in the decoupled-planes regime, A would be well approximated by the value $A = 3300$ sec^{-1} (Ref. 31) appropriate to La_2CuO_4, while if it were in the coupled-planes regime we would expect $A = 800$ sec^{-1}. [In fact, the values might be slightly larger since the J for $YBa_2Cu_3O_{6.0}$ is smaller than the J for La_2CuO_3 (Ref. 32).] In fact, in $YBa_2Cu_4O_8$, $A = 1600$ sec^{-1} (Ref. 24) compatible with neither estimate. An alternative argument would be to say that A_{QP} has the dimension of energy, and the characteristic energy scale is given by dividing the velocity v by the lattice constant a, implying $A \sim 1/v$, and so from Eq. (5.1) we would expect that in the coupled-planes regime the value of the Cu T_1 would come out about right. A third possibility is that for some unknown reason A_{QP} could drop by a factor of 8 upon going from $La_{2-x}Sr_xCuO_4$ to $YBa_2Cu_4O_8$, so that the data for $T > 150$ K would be consistent with the decoupled-planes regime. Of course a fourth possibility is that the theory is not applicable. Neutron measurements of absolute scattering intensities on underdoped YBa materials would be very helpful in resolving this issue.

Our discussion so far has emphasized properties related to the antiferromagnetic fluctuations. These are in a sense robust and relatively model independent, depending as they do primarily on the existence of a growing correlation length, a weak J_2, and a spin gap at low T. We now consider small-q properties. In the Heisenberg model, the behavior of the small-q susceptibility is very closely tied to the behavior of the large-q susceptibility.[11,33] In a more Fermi-liquid-like model this need not be true, and therefore the bilayer coupling, which strongly affects the behavior near the antiferromagnetic point, need not in a more realistic model also strongly affect the susceptibility near $q = 0$. It is also clear that the spin-only model is not, by itself, a reasonable description of the small-q spin dynamics of $YBa_2Cu_3O_{7-\delta}$ or $YBa_2Cu_4O_8$. For example, the observed yttrium nuclear relaxation rate does

not vary as T^2 but is more nearly proportional to the static susceptibility.[6] Also, our calculated oxygen nuclear relaxation rate is too small by about a factor of 16 to explain the data.[34] Thus, we must invoke an extra contribution to χ'' existing at least at small q. It is natural to suppose that this is due to the mobile carriers and that therefore the contribution to χ'' is of more or less the Fermi-liquid form. However, the Fermi-liquid-like contribution cannot be appreciable near the antiferromagnetic point or it would overdamp the spin waves and change the universality class of the magnetic fluctuations.[13,14] It has very recently been argued[35] that in the Shraiman-Siggia model of doped antiferromagnets[36] precisely the required behavior occurs, with the fermions making an additive contribution to the small-q but not the large-q susceptibilities. A similar conclusion was drawn from high-temperature series expansions.[29] In the resulting two-component picture $\chi=\chi_{\rm spin}+\chi_{\rm QP}$, with the Fermi-liquid like piece $\chi_{\rm QP}$ providing the yttrium and oxygen relaxation and the $\chi_{\rm spin}$ given by the theory we have discussed and providing the nontrivial temperature dependence of the uniform susceptibility and the Cu relaxation rate. Sokol and co-workers have made a similar argument on phenomenological grounds, claiming that the temperature dependence of χ in $YBa_2Cu_4O_8$ for 200 K $\leq T \leq$ 700 K is consistent with the behavior of the spin-only model in the quantum critical regime.[9] Now whether one supposes the material to be in the coupled-planes or decoupled-planes critical regime, the theory implies $\chi(T)=a+bT$. We ignore the value of a, on the grounds that it is dominated by the fermions which are beyond the scope of the theory, and consider the value of b, which is given by Eq. (4.3). From Eq. (5.1) assuming $g\mu_B$ takes the same value as in La_2CuO_4 we find $b=5\times10^{-3}$ states/eV Cu K for the decoupled-planes regime and $b=2.5\times10^{-3}$ states/eV Cu K for the coupled-planes regime. The data say that $b\sim1.6\times10^{-3}$ states/eV Cu K.[37] This too weak T dependence of χ in the critical regime suggests to us that the straightforward two-component approach is not applicable to $YBa_2Cu_4O_8$, and that the presence of carriers modifies the magnetic behavior more dramatically. We note, however, that two results which seem to be qualitatively consistent with the calculations presented here are the following: (a) Although the difference is not dramatic, the yttrium rate seems to drop faster than the oxygen rate as T is lowered and (b) the magnitude of the yttrium rate is larger than expected from a model in which the planes are uncoupled.[38]

Whatever is the correct theory, the distinction we have drawn between the coupled-planes and the decoupled-planes regimes will still be important. Further, if the NMR and neutron data on underdoped YBa superconductors are both taken at face value, then the crossover between the coupled-planes and decoupled-planes regimes occurs either at $T>700$ K or at $T\sim200$ K. The larger value seems to us to require an implausibly large between-planes coupling; the smaller value would imply that the crossover to the quantum disordered regime is complicated by a simultaneous freezing out of the optic mode of the bilayer system.

ACKNOWLEDGMENTS

H.M. was supported in part by the NSF under Grant No. PHY89-04035. We thank D. Pines and A. V. Sokol for helpful discussions and for preprints of their work. A.J.M. thanks P. C. Hohenberg for a helpful discussion concerning amplitude ratios and R. E. Walstedt for a critical reading of the manuscript. The authors thank the Correlated Electron Theory Program at Los Alamos National Laboratory for hospitality while part of the manuscript was written.

APPENDIX A: DERIVATION OF MEAN-FIELD EQUATIONS

We begin from Eq. (1.1). We write the model as a functional integral, introduce a field $Q^{(a)}_{\langle i,j\rangle}$ to decouple the J_1 interaction, a field Δ_i to decouple the J_2 interaction, and a field μ to enforce the constraint. We find for the partition function Z,

$$Z=\int \mathcal{D}\Delta^{+}\Delta\mathcal{D}Q^{+}Q\mathcal{D}b^{\dagger}b\mathcal{D}\mu\exp\left[-\int_0^{\beta}d\tau\mathcal{L}'\right], \tag{A1}$$

with

$$\begin{aligned}\mathcal{L}'=&\sum_{ia}b^{\dagger(a)}_{ia}[\partial_\tau+\mu^{(a)}_i]b^{(a)}_{ia}\\&+\frac{1}{4}\sum_{\langle i,j\rangle,a\alpha}b^{\dagger(a)}_{i\alpha}b^{\dagger(a)}_{j\alpha}Q^{(a)}_{\langle i,j\rangle}+\text{H.c.}\\&+\sum_{i\alpha}b^{\dagger(1)}_{i\alpha}b^{\dagger(2)}_{i\alpha}\Delta_i+\text{H.c.}\\&+\sum_{\langle i,j\rangle a}\frac{|Q^{(c)}_{\langle i,j\rangle}|^2}{8J_1}+\sum_i\frac{2|\Delta_i|^2}{J_2}\,.\end{aligned} \tag{A2}$$

The different normalizations of Q and Δ have been introduced, so that the final expression for the boson energy, Eq. (A9), has no numerical factors. We next introduce symmetric (s) and antisymmetric (a) Bose fields via

$$b^{(1)}_{k\alpha}=\frac{1}{\sqrt{2}}(s'_{k\alpha}+a'_{k\alpha})\,, \tag{A3a}$$

$$b^{(2)}_{k\alpha}=\frac{1}{\sqrt{2}}(s'_{k\alpha}-a'_{k\alpha})\,. \tag{A3b}$$

We make the mean-field approximation of space and time independent Q,Δ,μ, Fourier transform the boson operators, and obtain

$$\begin{aligned}\mathcal{L}_{\mathcal{B}}=&\sum_{k\alpha}s'^{\dagger}_{k\alpha}[\partial_\tau+\mu]s'_{k\alpha}+\left[\frac{1}{2}(Q\gamma_k+\Delta)s'^{\dagger}_{k\alpha}s'^{\dagger}_{-k\alpha}+\text{H.c.}\right]\\&+\sum_{k\alpha}a'^{\dagger}_{k\alpha}[\partial_\tau+\mu]a'_{k\alpha}+\left[\frac{1}{2}(Q\gamma_k-\Delta)a'^{\dagger}_{k\alpha}a'^{\dagger}_{-k\alpha}\right.\\&\left.+\text{H.c.}\right],\end{aligned} \tag{A4}$$

with

$$\gamma_k=\tfrac{1}{2}(\cos k_x+\cos k_y)\,. \tag{A5}$$

The boson part of this equation may be decoupled by a

Bogoliubov transformation. The resulting quasiparticles s and a are defined by

$$s'^{\dagger}_{k\alpha}=\cosh\theta_k s^{\dagger}_{k\alpha}-\sinh\theta_k s_{-k,\alpha}\ ,$$
$$a'^{\dagger}_{k\alpha}=\cosh\theta_{k+P} a^{\dagger}_{k\alpha}+\sinh\theta_{k+P} a_{-k,\alpha}\ , \tag{A6}$$

with

$$\tanh 2\theta_k=[Q\gamma_k+\Delta]/\mu \tag{A7}$$

and

$$P=(\pi,\pi)\ . \tag{A8}$$

The energy of the s bosons is

$$\omega_k=\sqrt{\mu^2-(Q\gamma_k+\Delta)^2}\ . \tag{A9}$$

The energy of an a boson at a wave vector k is ω_{k+P}.

The free energy F may be computed in the standard way and is

$$F=4NT\sum_k \ln[2\sinh(\omega_k/2T)]+NQ^2/2J_1 +2N\Delta^2/J_2-2N(1+2S)\mu\ . \tag{A10}$$

The mean field equations, Eqs. (2.9), follow from differentiating this equation with respect to μ, Q, and Δ.

APPENDIX B: APPROXIMATE SOLUTION OF MEAN-FIELD EQUATIONS

We begin with Eqs. (2.9). We recast them as $\int d^2k/(2\pi)^2\rightarrow\int d\gamma N(\gamma)$, we replace $N(\gamma)$ by $\frac{1}{2}$, and we normalize Q and Δ by μ and integrate, obtaining at $T=0$

$$\frac{\sin^{-1}(\Delta+Q)-\sin^{-1}(\Delta-Q)}{2Q}=1+2S\ , \tag{B1a}$$

$$\frac{\sin^{-1}(\Delta+Q)-\sin^{-1}(\Delta-Q)+(\Delta-Q)\sqrt{1-(\Delta+Q)^2}-(\Delta+Q)\sqrt{1-(\Delta-Q)^2}}{4Q^2}=\frac{Q\mu}{2J_1}\ , \tag{B1b}$$

$$\frac{\sqrt{1-(\Delta-Q)^2}-\sqrt{1-(\Delta+Q)^2}}{2Q}=\frac{2\Delta\mu}{J_2}\ . \tag{B1c}$$

These three equations may be reduced to one by taking the sine of Eq. (B1a) and substituting into Eq. (B1b) to obtain an equation for $\mu(Q)$, solving Eq. (B1c) to obtain an equation for $\Delta(Q)$, and then substituting the results into Eq. (B1b). However, for our purposes a simpler approach suffices. We first locate the critical point at which the minimum boson energy vanishes. In the notation of this appendix this implies $\Delta^*+Q^*=1$ (we denote by $*$ the values of the quantities at the critical point). Then Eq. (B1a) may be solved for Q^*. For $S>S_c=(\pi/2-1)/2$ this has only one solution; e.g., at $S=\frac{1}{2}$

$$Q^*\cong 0.277\ . \tag{B2}$$

For $S^*<S<S_c$, with $S^*\cong 0.19$ there are two solutions, one at Q near 1 which is the lower energy solution for $J_1\gg J_2$ and one at Q near $\frac{1}{2}$ which is the lower energy solution for J_1 near $J_2/4$. For $S<S^*$ there are no solutions.

Once a solution for Q^* is found, Eq. (B1c) implies

$$\frac{\mu^*}{J_2}=\frac{1}{2\sqrt{Q^*(1-Q^*)}} \tag{B3}$$

and Eq. (B1b) implies

$$\frac{J_2^*}{J_1^*}=2\frac{(1+2S)\sqrt{Q^*(1-Q^*)}-1+Q^*}{Q^{*2}}\ . \tag{B4}$$

Solving Eq. (B1a) and then using the solution in Eq. (B4) yields the phase diagram given in Fig. 2.

We now consider the $T>0$ behavior. We are most interested in the regime near the phase boundary, and in small J_2. We therefore solve the equations perturbatively in the small parameters S_c-S, J_2/J_1, and T. We neglect terms of third order and higher in these small parameters. To this order the T-dependent terms may be evaluated exactly. The equations are conveniently expressed in terms of the variables ω_+, ω_-, and μ and are (note we need μ only to first order in the small parameters),

$$\frac{\pi-\omega_+/\mu-\omega_-/\mu+(2T/\mu)[f(\omega_+/T)+f(\omega_-/T)]}{2[1-\omega_+^2/(4\mu^2)-\omega_-^2/(4\mu^2)]}=1+2S\ , \tag{B5a}$$

$$\frac{\pi-\omega_-/\mu-\omega_+/\mu+(2T/\mu)[f(\omega_+/T)+f(\omega_-/T)]}{4}=\frac{\mu}{2J_1}\ , \tag{B5b}$$

$$\omega_--\omega_++2T[f(\omega_+/T)-f(\omega_-/T)]=\frac{\omega_-^2-\omega_+^2}{J_2}\ . \tag{B5c}$$

Here the function f is defined by

$$f(x)=-\ln[1-e^{-x}] . \tag{B6}$$

We use Eq. (B5b) to solve for μ. Substituting and rearranging gives

$$\omega_+ +\omega_- -2T[f(\omega_+/T)+f(\omega_-/T)]-\frac{\omega_+^2+\omega_-^2}{j}=\epsilon , \tag{B7a}$$

$$\omega_- -\omega_+ -2T[f(\omega_-/T)-f(\omega_+/T)]=\frac{\omega_0^2-\omega_+^2}{J_2} , \tag{B7b}$$

with

$$j=2J_1[1+8(S_c-S)/\pi] \tag{B8}$$

and

$$\epsilon=\frac{2\pi J_1(S_c-S)}{1+8(S_c-S)/\pi} . \tag{B9}$$

These two equations may be easily solved numerically for ω_+ and ω_- by adding the two equations to obtain an expression for ω_+ in terms of ω_- and T, and then substituting that into one of the two equations to get a single equation for ω_-. At low T and sufficiently close to the phase boundary the equations have two solutions, one with $\omega_+<\omega_-$ and one with $\omega_+=\omega_-$; above a critical temperature the two solutions merge. By substituting the results in to Eq. (A9) we have verified that where the solution with $\omega_+<\omega_-$ exists it has a lower energy than the solution with $\omega_+=\omega_-$. The results displayed in the right panel of Fig. 3 were obtained in this manner.

APPENDIX C: SUSCEPTIBILITIES AND RELAXATION RATES

We begin with the dynamic susceptibilities, which we obtain by computing the linear response of the system to an externally applied magnetic field $\mathbf{h}_i^{(a)}$. The Schwinger-boson formalism is rotationally invariant. We therefore compute only the response to a field in the z direction. Thus we add to the Hamiltonian a term

$$\Delta H=\sum_{ia}\mathbf{h}_i^{z(a)}\cdot\mathbf{S}_i^{(a)} . \tag{C1}$$

After using Eqs. (2.2), (2.3), and (A3) this becomes

$$\Delta H=\sum_q \frac{h_q^{(1)}-h_q^{(2)}}{2}O_q^a+\frac{h_q^{(1)}+h_q^{(2)}}{2}O_q^s , \tag{C2}$$

with

$$O_q^a=\sum_{k\alpha\beta}\cosh(\theta_{k+q+P}+\theta_k)(s_{k+q+P\alpha}^{\dagger}\sigma_{\alpha\beta}^z s_{k\beta}+a_{k+q+P\alpha}^{\dagger}\sigma_{\alpha\beta}^z a_{k+q\beta})$$
$$+\sinh(\theta_{k+q+P}+\theta_k)(s_{k+q+P\alpha}^{\dagger}\sigma_{\alpha\beta}^z s_{-k\beta}^{\dagger}+\text{H.c.}+a\rightarrow s) , \tag{C3a}$$

$$O_q^s=\sum_{k\alpha\beta}\cos(\theta_{k+q}-\theta_k)(s_{k+q\alpha}^{\dagger}\sigma_{\alpha\beta}^z a_{k+P\beta}+a_{k+q\alpha}^{\dagger}\sigma_{\alpha\beta}^z s_{k+p\beta}+\text{H.c.})$$
$$+\sinh(\theta_{k+q}-\theta_k)(s_{k+q\alpha}^{\dagger}\sigma_{\alpha\beta}^z a_{-k-P\beta}^{\dagger}+a_{k+q\alpha}^{\dagger}\sigma_{\alpha\beta}^z s_{-k-\beta}^{\dagger}+\text{H.c.}) . \tag{C3b}$$

The only nonzero correlation functions are

$$\chi_q^{aa}(\omega)=\int_0^{\infty}dt e^{i(\omega+i\epsilon)t}\langle[O_q^a(t),O_{-q}^a(0)]\rangle$$
$$=4\sum_k\cosh^2(\theta_{k+q+P}+\theta_k)\frac{b(\omega_k)-b(\omega_{k+q+P})}{\omega-\omega_k+\omega_{k+q+P}+i\epsilon}$$
$$+4\sum_k\sinh^2(\theta_{k+q+P}+\theta_k)\frac{[1+b(\omega_k)+b(\omega_{k+q+P})](\omega_k+\omega_{k+q+P})}{(\omega_k+\omega_{k+q+P})^2-(\omega+i\epsilon)^2} \tag{C4a}$$

and

$$\chi_q^{ss}(\omega)=\int_0^{\infty}dt e^{i(\omega+i\epsilon)t}\langle[O_q^S(t),O_{-q}^S(0)]\rangle$$
$$=4\sum_k\cosh^2(\theta_{k+q}-\theta_k)\frac{b(\omega_k)-b(\omega_{k+q})}{\omega-\omega_k+\omega_{k+q}+i\epsilon}+4\sum_k\sinh^2(\theta_{k+q}-\theta_k)\frac{[1+b(\omega_k)+b(\omega_{k+q})](\omega_k+\omega_{k+q})}{(\omega_k+\omega_{k+q})^2-(\omega+i\epsilon)^2} . \tag{C4b}$$

We are interested in low energy phenomena; this implies that k and $k+q+P$ are near 0 or P. In this case we may approximate

$$\cosh(\theta_k)=(\mu/2\omega_k)^{1/2}(1+\omega_k/2\mu) , \tag{C5}$$

$$\sinh(\theta_k)=\mathrm{sgn}(\gamma_k)(\mu/2\omega_k)^{1/2}(1-\omega_k/2\mu) . \tag{C6}$$

Then near $q=0$ we have

$$\chi_q^{ss}(\omega)=\sum_k \frac{(\omega_k+\omega_{k+q})^2}{\omega_k\omega_{k+q}}\frac{b(\omega_k)-b(\omega_{k+q})}{\omega-\omega_k+\omega_{k+q}+i\epsilon}+\sum_k \frac{(\omega_k-\omega_{k+q})^2}{\omega_k\omega_{k+q}}\frac{[1+b(\omega_k)+b(\omega_{k+q})](\omega_k+\omega_{k+q})}{(\omega_k+\omega_{k+q})^2-(\omega+i\epsilon)^2}, \tag{C7}$$

$$\chi_q^{aa}(\omega)=\sum_k \frac{(\omega_k+\omega_{k+q+P})^2}{\omega_k\omega_{k+q+P}}\frac{b(\omega_k)-b(\omega_{k+q+P})}{\omega-\omega_k+\omega_{k+q+P}+i\epsilon}$$
$$+\sum_k \frac{(\omega_k-\omega_{k+q+P})^2}{\omega_k\omega_{k+q+P}}\frac{[1+b(\omega_k)+b(\omega_{k+q+P})](\omega_k+\omega_{k+q+P})}{(\omega_k+\omega_{k+q+P})^2-(\omega+i\epsilon)^2}, \tag{C8}$$

while near $q=P$

$$\chi_q^{ss}(\omega)=4\sum_k \frac{\mu^2}{\omega_k\omega_{k+q}}\left[\frac{b(\omega_k)-b(\omega_{k+q})}{\omega-\omega_k+\omega_{k+q}+i\epsilon}+\frac{[1+b(\omega_k)+b(\omega_{k+q})](\omega_k+\omega_{k+q})}{(\omega_k+\omega_{k+q})^2-(\omega+i\epsilon)^2}\right], \tag{C9}$$

$$\chi_q^{aa}(\omega)=4\sum_k \frac{\mu^2}{\omega_k\omega_{k+q+P}}\left[\frac{b(\omega_k)-b(\omega_{k+q+P})}{\omega-\omega_k+\omega_{k+q+P}+i\epsilon}+\frac{[1+b(\omega_k)+b(\omega_{k+q+P})](\omega_k+\omega_{k+q+P})}{(\omega_k+\omega_{k+q+P})^2-(\omega+i\epsilon)^2}\right]. \tag{C10}$$

In all of these formulas there are important contributions from k near 0 and k near P.

We now consider NMR. To derive nuclear relaxation rates we take the standard[2] hyperfine Hamiltonians describing how nuclei are coupled to the electronic spins, write the spins in terms of bosons, and then compute the appropriate boson correlation functions. We assume throughout that $T \ll J_1$.

We begin with the yttrium. An yttrium nucleus sits halfway between two nearest-neighbor CuO_2 planes and above the center of a plaquette formed by four Cu atoms. We denote the hyperfine coupling to one spin by D. Thus we write the hyperfine Hamiltonian for yttrium,

$$H_{\rm HF}^{\rm Y}=D\sum_{a,i=1,\ldots,4}\mathbf{S}_i^{(a)}. \tag{C11}$$

After performing the transformations of Sec. II and Appendix A and retaining only those terms capable of giving dissipation at NMR frequencies we have

$$H_{\rm HF}^{\rm Y}=D\sum_{k_1,q,\alpha,\beta} g(q)\times\cos(\theta_{k+q}-\theta_k)(s_{k+q\alpha}^{\dagger}\sigma_{\alpha\beta}a_{k+P\beta}+\text{H.c.}), \tag{C12}$$

with

$$|g(q)|=4\cos(q_x/2)\cos(q_y/2). \tag{C13}$$

Here we have omitted an unimportant phase factor in g. We now calculate the relaxation rate in the usual way, from

$$\lim_{\omega\to 0}\frac{1}{\omega}\int_0^{\infty} e^{i(\omega+i\epsilon)t}\langle[H_{\rm HF}^{\rm Y}(t),H_{\rm HF}^{\rm Y}(0)]\rangle, \tag{C14}$$

finding

$$\frac{1}{{}^{\rm Y}T_1T}=\frac{2\pi D^2}{T}\sum_{kq}\frac{|g(q)|^2\cosh^2(\theta_k-\theta_{k+q})\delta(\omega_k-\omega_{k+q})}{\sinh^2(\omega_k/2T)}$$
$$=2\pi D^2\lim_{\omega\to 0}\frac{1}{\omega}\sum_q |g(q)|^2\chi^{ss''}(q,\omega). \tag{C15}$$

We now consider the planar oxygen. Each oxygen is located in a CuO_2 plane and is in the center of a bond connecting two Cu sites. Thus

$$H_{\rm HF}^{\rm O}=C\sum_{i=1,2}\mathbf{S}_i^{(a)}. \tag{C16}$$

Expressing the spins in terms of bosons as was done for yttrium gives

$$H_{\rm HF}^{\rm O}=\frac{C}{2}\sum_{k,q} f(q)[\cosh(\theta_k+\theta_{k+q+P})(s_{k\alpha}^{\dagger}\sigma_{\alpha\beta}s_{k+q+P\beta}+a_{k+P\alpha}^{\dagger}\sigma_{\alpha\beta}a_{k+qb})+\cosh(\theta_k-\theta_{k+q})s_{k\alpha}^{\dagger}\sigma_{\alpha\beta}a_{k+q+P\beta}+\text{H.c.}], \tag{C17}$$

with

$$|f(k)|=2\cos\left[\frac{q_x}{2}\right].$$

Proceeding as we did with yttrium yields Eq. (3.10) of the text. To evaluate this it is convenient to consider q near 0 and q near P separately. The case of q near 0 goes through just as for yttrium, except that the square of the form factor is 4, not 16, and one must add $\chi^{aa''}$. For q near P it is convenient to write $q=P+k_2-k_1$ and to sum over k_1 and k_2. The integrals have contributions

from k_1, k_2 near 0 and P. The form factor becomes

$$|f(k_1-k_2)|^2=(k_1^x-k_2^x)^2=(k_1^2+k_2^2)/2 , \quad \text{(C18)}$$

where in the second equality we have done the angular integral and k stands for either k or $(k-P)$ as appropriate. Now we have, from Eqs. (A9) and (2.7),

$$k^2=4(1-\gamma_k)=2(\omega_k^2-\omega_{+,-}^2)/\mu^2 , \quad \text{(C19)}$$

where the gap is ω_+ for k near 0 and ω_- for k near P. Putting this into Eq. (3.10) yields Eq. (3.11). Finally, we consider the Cu relaxation rate. A Cu nuclear moment is believed to be coupled to the spin on the same site, via a hyperfine coupling A, and to the spins on the four nearest-neighbor sites in the same plane, via a hyperfine coupling B. Thus

$$H_{\rm HF}^{\rm Cu}=A\mathbf{S}_0^{(1)}+B\sum_{i=1,\ldots,4}\mathbf{S}_i^{(1)} . \quad \text{(C20)}$$

After transforming to the boson representation we have

$$H_{\rm HF}^{\rm Cu}=\frac{1}{2}\sum_{kq}[A-4B\gamma(q)][\cosh(\theta_k+\theta_{k+q+P})$$
$$\times(s_{k\alpha}^\dagger\sigma_{\alpha\beta}s_{k+q+P\beta}+a_{k\alpha}^\dagger\sigma_{\alpha\beta}a_{k+q+P\beta})$$
$$+\cosh(\theta_k-\theta_{k+q})s_{k+q\alpha}^\dagger\sigma_{\alpha\beta}a_{k+q+P\beta}+\text{H.c.}] . \quad \text{(C21)}$$

Again we may construct the relaxation rate. It is given by Eq. (3.12) and may be simply evaluated because the dominant contribution is at q near P.

*Present address: Theoretische Physik, ETH Hönggerberg, CH-8093 Zürich, Switzerland.

[1]T. Siegrist, S. Sunshine, D. W. Murphy, R. J. Cava, and S. M. Zahurak, Phys. Rev. B **35**, 7137 (1989).
[2]A. J. Millis, H. Monien, and D. Pines, Phys. Rev. B **42**, 167 (1991); H. Monien, D. Pines, and M. Takigawa, *ibid.* **43**, 258 (1991).
[3]J. Rossad-Mignod, L. P. Regnault, C. Vettier, P. Bourges, P. Burlet, J. Bossy, J. Y. Henry, and G. Lapertot, Physica C **185-189**, 86 (1991).
[4]J. M. Tranquada, P. M. Gehring, G. Shirane, S. Shamoto, and M. Sato, Phys. Rev. B **46**, 5561 (1992).
[5]H. A. Mook, M. Yethiraj, G. Aeppli, and T. Mason, Phys. Rev. Lett. **70**, 3490 (1993)
[6]M. Takigawa *et al.*, Phys. Rev. B **42**, 243 (1991).
[7]A. J. Millis and H. Monien, Phys. Rev. Lett. **70**, 2810 (1993).
[8]T. M. Rice, in *The Physics and Chemistry of Oxide Superconductors,* edited by Y. Iye and H. Yasuoka (Springer-Verlag, Berlin, 1992), p. 313.
[9]A. Sokol and D. Pines, Phys. Rev. Lett. **71**, 2813 (1993); V. Barzykin, D. Pines, A. V. Sokol, and D. Thelen, Phys. Rev. B **49**, 1544 (1994).
[10]S. Chakravarty, B. I. Halperin, and D. R. Nelson, Phys. Rev. Lett. **60**, 1057 (1988); Phys. Rev. B **39**, 7443 (1988).
[11]S. Sachdev and J. Ye, Phys. Rev. Lett. **69**, 2411 (1992); A. V. Chubukov and S. Sachdev, Phys. Rev. Lett. **71**, 169 (1993).
[12]N. W. Preyer, R. J. Birgeneau, C. Y. Chen, D. Gabbe, H. P. Jensen, M. A. Kastner, P. J. Picone, and T. Thio, Phys. Rev. B **42**, 11 563 (1989).
[13]J. A. Hertz, Phys. Rev. B **14**, 1165 (1976).
[14]A. J. Millis, Phys. Rev. B **48**, 7183 (1993).
[15]D. Arovas and A. Auerbach, Phys. Rev. B **38**, 316 (1988).
[16]S. Sachdev and N. Read, Int. J. Mod. Phys. B **5**, 219 (1991).
[17]K. Hida, J. Phys. Soc. Jpn. **61**, 1013 (1992).
[18]A. Sandvik and D. J. Scalapino, Phys. Rev. Lett. **72**, 2777 (1994).
[19]A. V. Chubukov, Phys. Rev. B **44**, 12 318 (1991).
[20]S. Chakravarty, in *High Temperature Superconductivity: Proceedings,* edited by K. Bedell, D. Coffey, D. E. Meltzer, D. Pines, and J. R. Schrieffer (Addison-Wesley, Redwood City, CA, 1990), p. 179; S. Chakravarty and R. Orbach, Phys. Rev. Lett. **64**, 224 (1990).
[21]P. Peczak, A. M. Ferrenberg, and D. P. Landau, Phys. Rev. B **43**, 6087 (1991).
[22]D. Forster, D. R. Nelson, and M. Stephen, Phys. Rev. A **16**, 732 (1977).
[23]C. H. Pennington and C. P. Slichter, Phys. Rev. Lett. **66**, 381 (1991).
[24]T. Machi, I. Tomeno, T. Miyatake, N. Koshizuka, S. Tanaka, T. Imai, and H. Yasuoka, Physica C **173**, 32 (1991).
[25]W. E. Pickett, Rev. Mod. Phys. **61**, 433 (1991); see especially Sec. IV-D and Fig. 30.
[26]R. Liu, B. W. Veal, A. P. Paulikas, J. W. Downey, P. J. Kostic, S. Fleshler, U. Welp, C. G. Olson, X. Wu, A. J. Arko, and J. Joyce, Phys. Rev. B **46**, 11 056 (1992).
[27]For T_2, M. Takigawa *et al.* (unpublished); for T_1 see Ref. 6.
[28]T. Imai, C. P. Slichter, K. Yoshimura, M. Katoh, and K. Kosuge, Phys. Rev. Lett. **71**, 1254 (1993).
[29]R. Glenister, R. R. P. Singh, and A. Sokol, Phys. Rev. Lett. **72**, 1549 (1994).
[30]S. Hayden, G. Aeppli, R. Osborn, A. D. Taylor, T. G. Perring, S. W. Cheong, and Z. Fisk, Phys. Rev. Lett. **67**, 3622 (1991).
[31]T. Imai, C. P. Slichter, K. Yoshimura, and K. Kosuge, Phys. Rev. Lett. **70**, 1002 (1993).
[32]There is some disagreement in the literature about the value of J appropriate to $YBa_2Cu_3O_{6.0}$. The estimate 0.1 eV $< J <$ 0.12 eV is given in Sec. 2.3 of a recent review [D. C. Johnston, Magn. Magn. Mater. **100**, 218 (1991)]. The J value for La_2CuO_4 is 0.13 eV.
[33]D. Forster, *Hydrodynamic Fluctuations, Broken Symmetry and Correlation Functions* (Benjamin Cummings, Reading, PA, 1975).
[34]A. J. Millis and H. Monien, Phys. Rev. B **45**, 3059 (1992). Hyperfine couplings are given in a convenient dimensionless form in Table I of this work, and the observed ratio of Cu to O relaxation rates in $YBa_2Cu_3O_{6.6}$ at $T=300$ K is quoted to be 16; we assume the ratio is similar in $YBa_2Cu_4O_8$. The quantity defined here as $A_{\rm AF}$ is related to B in Table I of the cited work via $A_{\rm AF}=4B(1-\alpha)/(1+\alpha)$. The bounds $0.2<\alpha<0.3$ were obtained from data in this work also. The

quantity defined here as C_{AF} is actually a tensor with different principal axes along and perpendicular to the Cu-O bond. For the estimates used here we set $C_{AF}=C$ and took the value for fields along the Cu-O bond (as appropriate for relaxation with fields in the c direction). The ratio A_{AF}/C_{AF} then turns out to be 4, and so at $T=300$ K where the predicted $\xi=4$ the predicted ratio is about 256.

[35]S. Sachdev and A. V. Chubukov, Phys. Rev. Lett. **71**, 169 (1993).

[36]B. I. Shraiman and E. D. Siggia, Phys. Rev. B **42**, 2485 (1990).

[37]H. Zimmermann, M. Mali, M. Bankay, and D. Brinkmann, Physica C **185-189**, 1145 (1991). The relevant data are in Fig. 3. To convert Knight shifts to susceptibilities we used the hyperfine couplings given in Ref. 34 for $YBa_2Cu_3O_7$ with the quantity χ_0/μ_B^2 of Ref. 34 taken to be 2.7 states/eV Cu.

[38]M. Takigawa, J. L. Smith, and W. Hults, Phys. Rev. Lett. **71**, 2650 (1993).